

Predictive Liquid Chromatography Separation for Mixtures of Functionalized Double-Decker Shaped Silsesquioxanes Based on HPLC Chromatograms

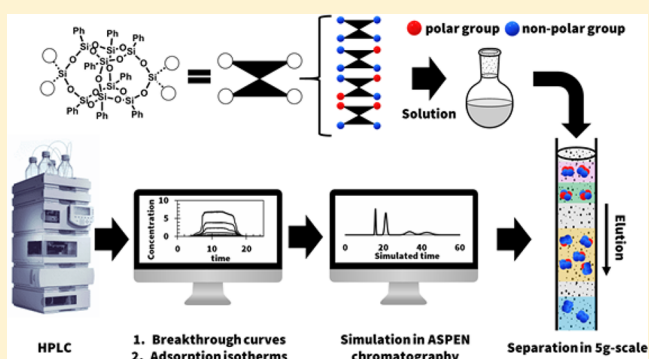
David F. Vogelsang,[†] Robert E. Maleczka, Jr.,^{*,‡,†} and Andre Lee^{*,†,‡}

[†]Department of Chemical Engineering and Materials Science, Michigan State University, Engineering Building, 428 South Shaw Lane, Room 2100, East Lansing, Michigan 48824-1226 United States

[‡]Department of Chemistry, Michigan State University, 578 South Shaw Lane, East Lansing, Michigan 48824-1322 United States

S Supporting Information

ABSTRACT: Analytical separation parameters of a side-capped octaphenyl double-decker shaped silsesquioxanes (DDSQ) mixture with zero, one, and two hydroxyl groups were obtained with HPLC. These parameters were extrapolated for a large scale preparative separation. The frontal analysis was experimentally performed for each component in the mixture to obtain linear adsorption isotherm parameters. The slopes of the linear isotherms were related with the experimental HPLC retention times in a linear function to predict separation for other mixtures with similar characteristics. The HPLC chromatograms were simulated in ASPEN chromatography with acceptable accuracy. Parameters of the scale-up separation were determined and prediction of collection times for each compound in three different mixtures was evaluated by separations using 5 g scale. Most importantly, scale-up isolation of chemically asymmetric DDSQ structure was demonstrated.



1. INTRODUCTION

Functionalized DDSQ structures can be obtained by reacting tetrasilanol octaphenyl double-decker shaped silsesquioxane (DDSQ-(Ph)₈(OH)₄) **1** with functional chlorosilanes.^{1–14} When two equivalents of difunctional dichlorosilanes (R₁R₂SiCl₂) are used, generally a closed structure (DDSQ-2(R₁R₂)) is obtained.^{3,5,14–16} DDSQ-2(R₁R₂) has been explored for different applications such as amphiphilic molecules in Langmuir–Blodgett films,¹⁷ ionic liquids,⁵ or support for heterogeneous catalyst.^{18,19} In addition, there are numerous studies using DDSQ-2(R₁R₂) in hybrid inorganic–organic polymers as the resultant hybrid polymers will contain the nanostructure as a part of the chain backbone.^{5,10,12,13,20–23} These hybrid polymers have shown enhanced hydrophobic properties,^{10,12,21} low dielectric constants,^{12,22,24} and improved thermo-oxidative stability without sacrifice of their mechanical performance.^{11–13,20}

Recently, our group synthesized several mixtures of DDSQ structures functionalized with zero, one, and two hydroxyl groups. These mixtures were synthesized by capping the DDSQ-(Ph)₈(OH)₄ with 1 mol equiv of (CH₃)(R)SiCl₂ and 1 mol equiv of methyl-trichlorosilane (CH₃)SiCl₃ followed by hydrolysis.²⁵ The structure with a single hydroxyl group, DDSQ-(CH₃R)(CH₃OH), was recognized as an asymmetric structure. Separation of this asymmetric structure from the

mixture was achieved with an optimal resolution of the elution by the use of adsorption HPLC.²⁵

In this work, we denoted the asymmetric structure with the general formula (DDSQ-(R₁R₂)(R₃OH)). To further explore engineering applications of asymmetric DDSQ structures, development of large-scale separation methodology to remove the symmetric byproducts is required. Scaling up adsorption HPLC separations to preparative liquid chromatography (LC) requires the use of a different stationary phase. This change usually represents large void volumes, high injection volume, and high concentrated injections, among other factors which may end-up decreasing the resolution of the elution.^{26,27} The scope of this paper was to simulate the separation of DDSQ-(R₁R₂)(R₃OH) from the mixture by HPLC. In modeling the HPLC column, breakthrough curves were performed by HPLC and analysis of the elution front permits obtention of the adsorption isotherm parameters for each compound in the mixture. Once the simulation converges with experimental chromatograms, extrapolation of the adsorption parameters can then be used to predict the collection time needed in a large scale preparative chromatography separation. This prediction allows a proper column configuration to achieve

Received: November 5, 2018

Accepted: December 12, 2018

Published: December 12, 2018

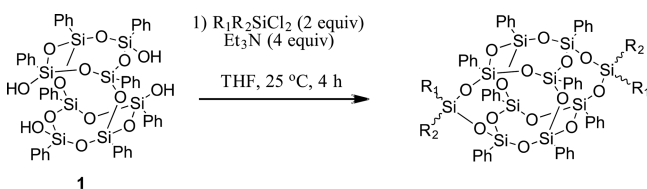
separations with resolutions of the elution large enough to isolate nearly pure asymmetrical compound.

2. EXPERIMENTAL SECTION

2.1. Materials. All commercially available chemicals were used as received unless otherwise indicated. $(C_6H_5)_8Si_8O_{10}(OH)_4$, 5,11,14,17-tetra(hydro)octaphenyltetracyclo[7.3.3.-3³.7]octasilsequioxane, or DDSQ-(Ph)₈(OH)₄ was purchased from Hybrid Plastics. Dimethyldichlorosilane $(CH_3)_2SiCl_2$, methyl trichlorosilane $(CH_3)SiCl_3$, vinyl trichlorosilane $(CH_2CH)SiCl_3$, isobutyl trichlorosilane $((CH_3)_2CHCH_2)SiCl_3$, and deuterated chloroform with 1% vol tetramethylsilane ($CDCl_3$ -1%TMS) were purchased from Sigma-Aldrich and from Gelest. Triethylamine (Et_3N) was purchased from Avantor. Tetrahydrofuran (THF) was dried passing through the alumina adsorbent column. Reagent grade dichloromethane (DCM) was degassed with helium for HPLC experiments. The previously listed solvents were purchased from Sigma. Si-gel P-60 was obtained from Silicycle. ¹H, ¹³C, and ²⁹Si were recorded on 500 MHz NMR spectrometers.

2.2. Methods. **2.2.1. Synthesis of DDSQ Individual Products.** DDSQ-2((CH₃)₂) **2** and DDSQ-2((CH₃)(OH)) **4a** were synthesized following Scheme 1. In a 500 mL flask

Scheme 1. Synthesis of Functionalized DDSQ-2(R₁)(R₂)^a

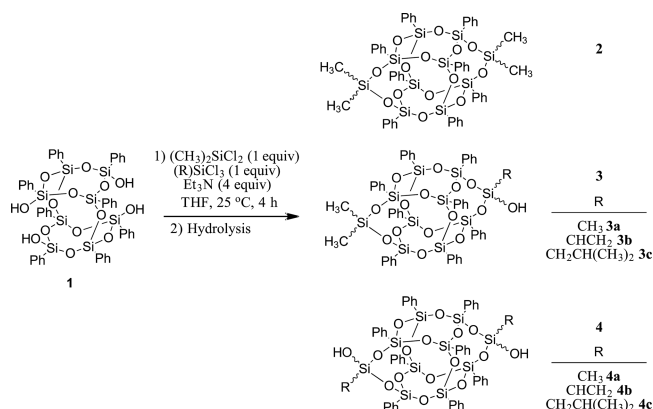


^aFor compound **2**: R₁ and R₂ are CH₃; for compound **4a**: R₁ is CH₃ and R₂ is Cl which is hydrolyzed after the reaction to form hydroxyl (OH).

purged with dry N₂ for 15 min, DDSQ-(Ph)₈(OH)₄ **1** (10 g, 9.35 mmol, 1 equiv) was dissolved in THF (200 mL) at room temperature. Dimethyldichlorosilane or methyl trichlorosilane (18.7 mmol, 2 equiv) was added to the DDSQ-(Ph)₈(OH)₄ **1** solution. Et₃N (37.4 mmol, 4 equiv) was added dropwise for a period of about 5 min to the stirring solution; a cloudy white suspension was formed and stirring was continued for an additional 4 h at room temperature. The solution was then filtered through a fine fritted-funnel-filter to remove the solid triethylamine hydrochloride. The volatiles were removed using a rotary evaporator. The sample was then solubilized in a minimum volume of DCM and then passed through a short silica-gel plug using DCM as a solvent to clean the sample and hydrolyze when methyl trichlorosilane was used. The volatiles were removed from the resulting solution and further dried at 0.4 mbar and 50 °C for 12 h to afford **2** or **4a** as white powders. Spectral information can be found in the [Supporting Information](#).

2.2.2. Synthesis of DDSQ Mixtures. The synthesis of DDSQ mixtures with zero, one, and two hydroxyl groups was performed following Scheme 2 using a procedure previously described.⁸ Synthesis of a mixture containing **2**, **3a**, and **4a** (or mixture **A**) is described as an example. To a 500 mL flask purged with dry N₂ for 15 min, **1** (10 g, 9.34 mmol) was added and dissolved in THF (200 mL) at room temperature. Dimethyldichlorosilane (9.34 mmol, 1.14 mL, 1 equiv) and methyl trichlorosilane (9.34 mmol, 1.10 mL, 1 equiv) were

Scheme 2. Synthesis of Mixtures Containing DDSQ-4(CH₃)₂, DDSQ-(CH₃)₂(R)(OH) **3, and DDSQ-2((R)(OH)) **4**, where R is Methyl (CH₃), Vinyl (CHCH₂), or Isobutyl (CH₂CH(CH₃)₂)**



added to the solution containing **1** and stirred for 5 min. Et₃N (37.4 mmol, 5.22 mL, 4 equiv) was added in 1 mL installments to the stirring solution. A cloudy white suspension was formed and stirred continuously for additional 4 h. The solution was filtered through a fine fritted-funnel-filter to remove the solid triethylamine hydrochloride. Volatiles were removed from the resulting solution which produced a white powder. The powder was dissolved in a minimum amount of DCM and hydrolyzed after addition of 50 mL of water and 1 h of stirring. The organic phase was isolated, washed with brine, and then dried with magnesium sulfate. The volatiles were evaporated ending with the mixture **A** as a white powder. Nearly pure **3a** was then isolated from the mixture **A** using LC. The same procedure was repeated replacing methyl trichlorosilane for vinyl trichlorosilane to produce the mixture **B** (**2**, **3b**, and **4b**), and for isobutyl trichlorosilane to produce the mixture **C** (**2**, **3c**, and **4c**). Spectral information for **3a**, **3b**, and **3c** cages can be seen in the [Supporting Information](#).

2.2.3. Breakthrough Curves. Breakthrough curves were generated in an Agilent 1100 HPLC system with a dual pump using a Lichrospher-Si60 column with an inner radius (*r*) of 0.23 cm and a length (*H_b*) of 25 cm. Analytes were detected with an UV-detector at 245 nm. Each compound was first solubilized in DCM with varying concentrations listed in [Table 1](#). The solution was pumped through pump A at a flow rate (*F_v*) of 1 mL/min for 10 min.; pure DCM was then pumped from pump B for 40 min with the same *F_v* for complete elution.

Adsorption isotherms were calculated using eq 1,²⁸ where the hold-up time (*t₀*) in the column used was found experimentally as 2.0 min. The extra column time (*t_{ext}*) was calculated based on the channels from the HPLC redirection valve to the beginning of the column and from the end of the column to the detector. For our HPLC, the value of *t_{ext}* was found to be 0.7 min experimentally. The shock time (*t_s*) was picked from the chromatogram as the half-time of the front located between the baseline and the beginning of the plateau after the detection of DDSQ compounds.

$$q_v = \frac{CF_v(t_s - t_0 - t_{ext})}{\pi H_b r^2 - F_v t_0} \quad (1)$$

The experimental adsorption isotherm was fitted to the linear isotherm model, eq 2.

Table 1. Solutions Prepared for Obtention of Breakthrough Curves^a

Compound	Concentration (C) (g/L)							
	1	2	3	4	5	6	7	8
2	0.10	0.18	0.30	0.40	1.06	1.60	2.20	
3a	0.09	0.19	0.33	0.57	0.98	1.83	2.82	6.25
4a	0.14	0.25	0.50	1.20	2.40	3.90	7.00	

^aConcentrations of 4a are for a 1:1 mixture of *cis* and *trans* isomers.

Table 2. Preparative Column Dimensions and Operational Parameters

Column	Preparative 1	Preparative 2	Preparative 3
Mixture	A (2, 3a, 4a)	B (2, 3b, 4b)	C (2, 3c, 4c)
Composition (2:3:4)	32:49:19	42:47:11	40:45:14
Height (H _b) cm	34	43	43
Radius (r) cm	1.7	3.4	3.4
Void fraction	0.7	0.6	0.6
Flow rate (mL/min)	25	54	19 to 87 for 10.4 min 87 to 103 for 13.0 min 54 to finish
Mixture weight (g)	2	4	4
Volume injected (mL)	15	46	46

$$q_p = IP1 * C + IP2 \quad (2)$$

where IP1 and IP2 are isotherm parameters and IP2 was fitted to be zero for all cases here.

2.3. HPLC and Preparative LC Chromatograms. HPLC experiments were configured using DCM as the mobile phase. The solvent was degassed with helium before pumping to the column. The flow rate was set to be 1 mL/min for all samples, which gave a constant pressure of 34 bar; the temperature was set as 25 °C, the injection volume was 10 μL, and the UV detector was set at 254 nm. The number of theoretical plates (*N*) or column efficiency was calculated with the tangent line method in eq 3. For HPLC, retention time (*t_r*) and peak width at the baseline (*W*) were calculated using the Agilent Chemstation software.²⁹ For preparative LC *t_r* and *W* were calculated manually from the plots. The resolution of the elution (*R_s*) was obtained using eq 4.

$$N = 16 \left(\frac{t_r}{W} \right)^2 \quad (3)$$

$$R_s = \frac{2(W_{(i)} + W_{(i+1)})}{(t_{r(i+1)} - t_{r(i)})} \quad (4)$$

Preparative LC was performed to scale-up the results obtained from HPLC experiments. Two different columns were prepared in the following general methodology. DCM was added to a dry silica bed inside a glass column. The formed slurry was shaken to remove most air bubbles. Then, the wet bed was flushed with DCM under pressure generated by a dry N₂ stream. The flushing process was stopped until the flow was constant in the column outlet, meaning that air was mostly removed from the column. Void fraction was calculated based on the volume required to elute an injection of toluene through the column at the average flow rate. A concentrated solution of DDSQ mixture dissolved in DCM was gently injected in the top of the wet Si-gel bed. The injection was flushed until no solution was observed above the packed bed. The column was then gently charged with DCM and the column pressurized by the N₂ stream to elute the analytes. Fractions were collected in the bottom of the column until the remaining DCM reached the top of the bed. The

concentration in each fraction was obtained by evaporation of the solvent and weighing the solid mass or by HPLC peak areas compared against a standard reference. Elution times in the preparative separation for mixtures A and B were calculated based on the relation between the volume of each fraction and the average flow rate. For the separation of mixture C, the flow rate for every collected fraction was recorded to analyze the effect of flow rate gradients in the simulation results. The dimensions of the columns and parameters for the separations performed can be observed in Table 2.

2.4. Chromatogram Simulation. ASPEN chromatography V10 was used to simulate the separation process in HPLC as well as in preparative LC. A batch process was drawn starting with an inlet controlling the mobile phase and the injection. This stream was connected to a packed column, and the column was further connected to an outlet stream. To start the modeling, trace-liquid was assumed for the column operation because the density of the liquid along the column is considered to be a constant. Two other assumptions in the mass balance are (1) no changes in flow rate (*F_v*); and (2) no additional reaction occurs during the separation process. After these assumptions, the resultant mass balance can be observed in eq 5.

$$\varepsilon_i E_{zi} \frac{\partial^2 C_i}{\partial z^2} = v_L \frac{\partial C_i}{\partial z} + \varepsilon_t \frac{\partial C_i}{\partial t} + (1 - \varepsilon_i) J_i \quad (5)$$

ε_t is the total void fraction which is a function of the interparticle void fraction ε_i and the intraparticle void fraction ε_p which is neglected here. C_i is the concentration of *i* molecule at a given time and position, and J_i is the mass transfer flux. E_{zi} stands for the axial dispersion coefficient. E_{zi} was calculated based on the theoretical column number of plates (*N*) described in eq 6, where H_b is the packed bed height.

$$E_{zi} = \frac{v_L H_b}{2N_p \varepsilon_i} \quad (6)$$

The linear lumped resistance assumption was made to obtain an expression for J_i (eq 7). Under this assumption, the mass transfer driving force for component *i* is a linear function of the liquid phase concentration.³⁰ In eq 7, q_i^* represents a

reference value for component i adsorbed. The mass transfer coefficient MTC was estimated by ASPEN assuming $0.005 \text{ cm}^2/\text{min}$ as standard value for molecular diffusivity in liquids.

$$J_i = \frac{dq_i}{dt} = \text{MTC}(q_i^* - q_i) \quad (7)$$

The system was divided into 500 nodes and further solved by finite differences using the quadratic upwind differencing scheme.

3. RESULTS AND DISCUSSION

3.1. Breakthrough Curves and Calculated Adsorption Isotherms. Breakthrough curves were obtained for 2, 3a, and 4a as observed in Figure 1. For 2, the shock times were the

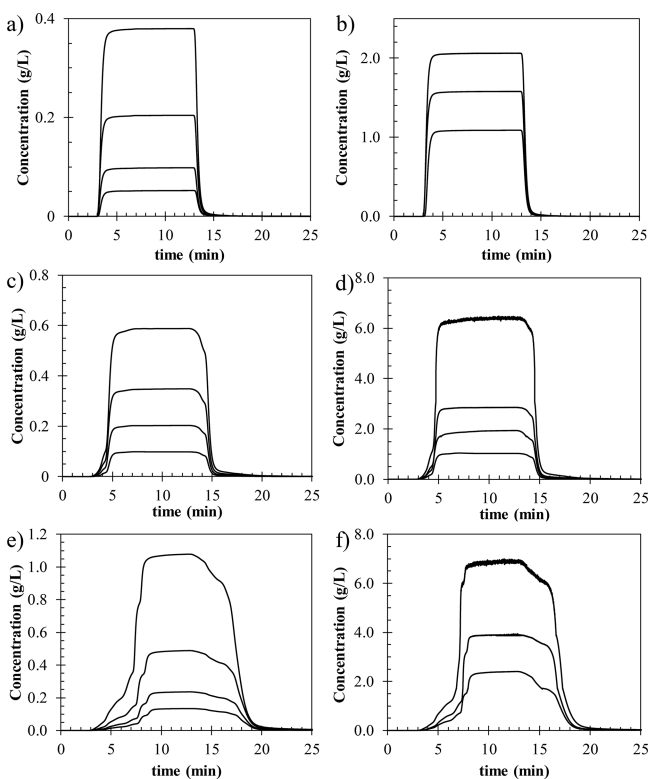


Figure 1. Breakthrough curves for (a) 2 in low concentrations, (b) 2 in high concentrations, (c) 3a in low concentrations, (d) 3a in high concentrations, (e) 4a in low concentrations, and (f) 4a in high concentrations. t_s was calculated from the half-concentration in the curve front.

same for all concentrations studied. This occurs as 2 is a molecule without silanol groups and its adsorption to the stationary phase is limited. Breakthrough curves for 3a showed a slight decrease in t_s when the concentrations were increased. The highly polar 4a exhibited a larger reduction in t_s as the concentration increases. Two fronts were observed for 4a corresponding to *trans*-4a and *cis*-4a. t_s was identified for each one of the fronts in 4a breakthrough curves. This observation enables the calculation for the adsorption behavior of each isomer and the prediction of *cis* and *trans* separation in the chromatogram simulation. The plateau region for concentrations higher than 10 g/L was above the detection limit. As a result, there was a breakdown of linearity between absorbance and concentration. This implies possible errors in the identification of t_s in the half concentration of the front. In

addition, samples at a concentration above 10 g/L had a tendency to form crystals within the HPLC pump pistons and block the flow in the column.

Experimental results for adsorption equilibrium followed a linear trend. Therefore, the isotherms were fitted with high accuracy into a linear adsorption isotherm model. Adsorption equilibrium data calculated using eq 1 and fitting of the data in the linear eq 2 are observed in Figure 2. The experimental IP1

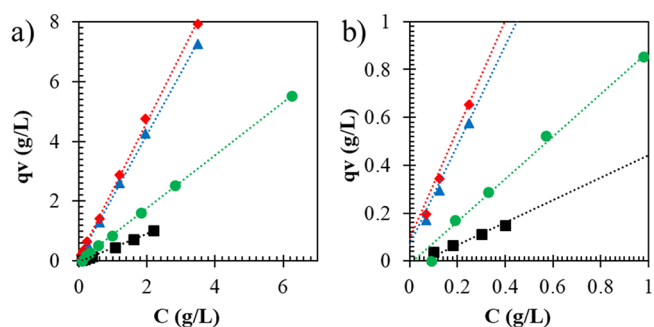


Figure 2. Experimental adsorption isotherms and linear fitting for: 2 black squares, 3a green circles, *trans*-4a blue triangles, and *cis*-4a red diamonds. (a) full experimental points; (b) low concentration points.

parameters calculated for HPLC separation for the components of mixture A were tabulated and shown in Table 3. Some

Table 3. Linear Adsorption Isotherm Parameter (IP1) Values Obtained Experimentally and Calculated Values

Compound	IP1 Experimental	IP1 for HPLC column calculated from eq 8	IP1 for preparative column calculated from eq 9
2	0.3753	0.3767	0.0645
3a	0.7940	0.7968	1.6288
<i>trans</i> -4a	1.9850	1.9816	6.0937
<i>cis</i> -4a	2.1822	2.1844	6.8329
3b		0.6899	1.2385
<i>trans</i> -4b		1.3026	3.5354
<i>cis</i> -4b		1.5248	4.3684
3c		0.5986	0.8963
<i>trans</i> -4c		0.9373	2.1660
<i>cis</i> -4c		1.1351	2.9077

of the effects for high concentrations in the chromatogram such as peak tailing or maximum adsorption capacity were not studied as DDSQ breakthrough curves cannot be obtained at high concentrations.

3.2. Simulation Results and Parameter Fitting. Based on the linear behavior of the adsorption isotherms for the components in mixture A, it was hypothesized that isotherms for mixtures B and C could also be linear. The isotherm parameter IP1 for each component in the mixture A was plotted against the retention time correspondent to each peak seen in Figure 3.

The relation between IP1 and t_r for mixture A was linear. For instance, eq 8 was calculated making a linear fitting. Equation 8 was used for calculation of the HPLC IP1 parameters ($IP1_{\text{HPLC}}$) for the components in the mixture B and in the mixture C. These parameters can be observed in Table 3. This approximation was made by taking into account the similarity of components in the mixtures, as well as the fact that differences in retention times between 4a, 4b, and 4c are

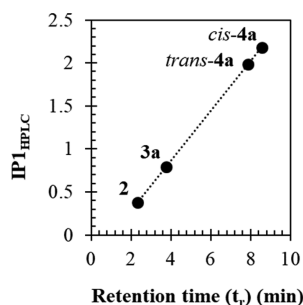


Figure 3. Linear behavior between the retention times (t_r) in HPLC and the linear isotherm parameter $IP1$ obtained from FA for mixture A.

mainly affected by the organic group adjacent to the hydroxyl group.³¹ The $IP1_{HPLC}$ values obtained were fed into the model, and the HPLC chromatograms for mixture A, for mixture B, and for mixture C were simulated as seen in Figure 4.

$$IP1_{HPLC} = 0.2901t_r - 0.2983 \quad (8)$$

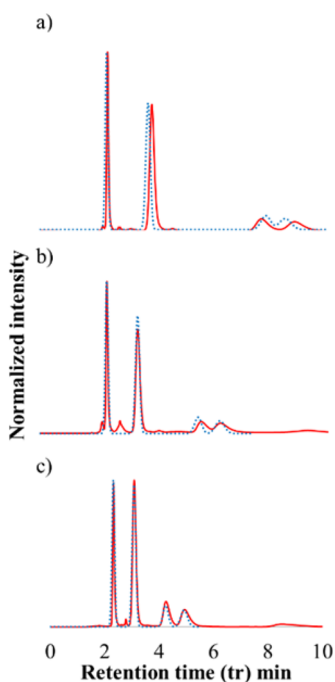


Figure 4. Curves in red represent the chromatograms obtained by HPLC. Curves in dotted blue lines represent the simulated chromatograms for (a) mixture A, (b) mixture B, and (c) mixture C.

3.3. Extrapolation of HPLC Parameters to Preparative Column. The stationary phase in the HPLC column is composed by $5 \mu\text{m}$ nonporous spherical silica particles densely packed in the column with void fraction around 0.1. On the other hand, the preparative column has silica as a stationary phase with particle size averaging $60 \mu\text{m}$, not homogeneous particle shape, and porous particles, and once packed in the column the void fraction can be higher than 0.5. Consequently, HPLC and preparative LC have different adsorption isotherm parameters. A glass column packed with Silicycle P-60 silica was prepared for separation of 2 g of the mixture A to obtain the preparatory LC parameters. Fractions of 9.5 mL were

collected and every fraction dried and weighed to elaborate the experimental chromatogram observed in Figure 5a.

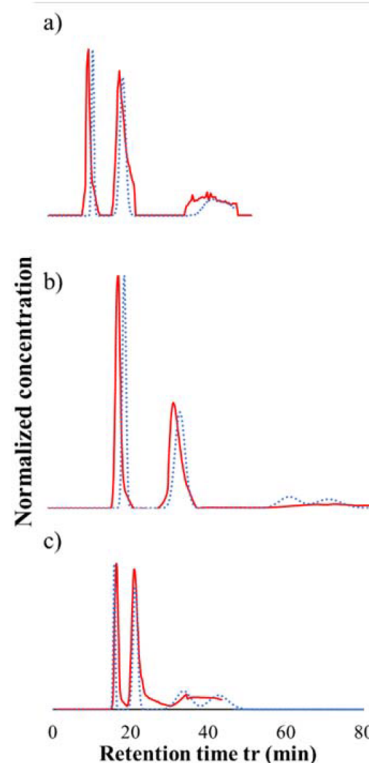


Figure 5. Curves in red represent the chromatograms obtained by preparative liquid chromatography. Curves in dotted blue lines represent the simulated chromatograms for (a) mixture A, (b) mixture B, and (c) mixture C.

Separation for mixture A was simulated by guessing the $IP1$ values in the model. The graph of $IP1$ against t_r in the preparative column followed a linear behavior like the one observed in the HPLC column. $IP1$ parameters from the HPLC column were correlated with $IP1$ parameters from the preparative column, obtaining the linear correlation observed in Figure 6 as well as in eq 9.

$$IP1_{prep} = 3.7488IP1_{HPLC} - 1.3477 \quad (9)$$

A preparative column was packed for separation of 5 g of mixture B and 5 g of mixture C to test the predictive model for columns with Silicycle P-60 silica. Simulation for separation of mixture B resulted in an accurate prediction for collection times for every compound. However, retention times were just

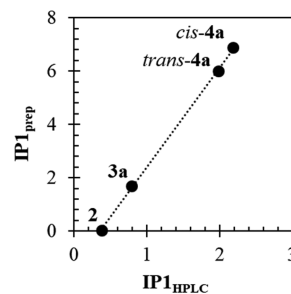


Figure 6. Relation between $IP1$ obtained from HPLC ($IP1_{HPLC}$) and $IP1$ obtained from preparative column ($IP1_{prep}$).

acceptably predicted. The experimental preparative chromatogram and the simulated chromatogram were compared and shown in Figure 5b. Analysis of each fraction was performed by HPLC and can be observed in the Supporting Information. Separation of mixture C was performed as follows: first, the flow rate was increased from 19 mL/min to 87 mL/min in a lapse of 10.4 min.; from 87 mL/min to 103 mL/min for 13 min; and then suddenly dropped to 54 mL/min for the remaining experiment. Experimental ramps were reposted in the Supporting Information. The separation using flow rate gradients was simulated, and the results obtained are in acceptable fitting with the experiment as seen in Figure 5c. On average, 85% of the initial weight was recovered after the separation process.

Prediction of separation between *cis* and *trans* molecules of 4 indicates that is possible to collect fractions enriched with the *cis* isomers and fractions enriched with the *trans* isomers. The predicted results agree with the experimental results showing that effectively *cis* and *trans* isomers of the DDSQ with two hydroxyl groups can be partially separated using DCM as the mobile phase. Previously separation of *trans* and *cis* DDSQ cages capped with isobutyl trichlorosilane was achieved in a silica column with toluene as mobile phase.¹⁷ Enriched fractions of *cis-4b*, *trans-4b*, *cis-4c*, and *trans-4c* can be observed in the HPLC analysis for preparative separations presented in the Supporting Information file.

3.4. Efficiency for Preparative Columns. Analysis of the column efficiency by eq 3 was used to estimate the dispersion coefficient by ASPEN chromatography. Table 4 contains the

Table 4. Column Efficiency (*N*) Calculated from Eq 3 for HPLC and Preparative Columns^a

Compound	<i>N</i> preparative-1	<i>N</i> preparative-2	<i>N</i> HPLC
2	261	603	7178
3a	191		2235
3b		430	2359
3c			2635
<i>trans-4a</i>	105*		1936
<i>cis-4a</i>			1694
<i>trans-4b</i>		212	697
<i>cis-4b</i>		217	853
<i>trans-4c</i>			1427
<i>cis-4c</i>			1117

^a* indicates value calculated as an individual component.

calculated column efficiencies for preparative-1, preparative-2, and HPLC. For compound 2, the difference in *N* values between preparative-1 and preparative-2 columns is mainly attributed to the larger diameter and length of preparative-2; larger column diameters generally reduce the injection height, decreasing the initial dispersion in the column. On the other hand, longer columns have a higher number of theoretical plates. The calculated efficiency for separation of 4b was half of 4a and 4c in HPLC due to overlapping of elution peaks. As seen in Table 4, the values of *N* for the preparative column are 1 order of magnitude smaller than the *N* for HPLC. Calculation of *N* for preparative columns has the same trend as the *N* calculated by HPLC.

In Table 5, values of resolution of the elution (R_s) calculated with eq 4 are tabulated. R_s between 2 and 3 and between 3 and 4 were higher than the optimal value, $R_{s-optimal} = 1.5$, in HPLC as well as in preparative LC. These R_s values indicate that every

Table 5. Resolution of the Elution between Analytes in Each Mixture after Separation by HPLC and Preparative LC

R_s between compounds	R_s by HPLC	R_s by Preparative LC
2 and 3a	7.1	2.1
2 and 3b	5.5	3.1
2 and 3c	4.3	1.8
3a and <i>trans-4a</i>	7.4	2.0
3b and <i>trans-4b</i>	3.9	2.9
3c and <i>trans-4c</i>	3.4	1.7
<i>trans-4a</i> and <i>cis-4</i>	1.5	
<i>trans-4b</i> and <i>cis-4b</i>	0.8	0.2
<i>trans-4c</i> and <i>cis-4c</i>	1.3	

analyte was eluted with high purity. In addition, further improvement may be made to reduce the separation time. Calculations of R_s for HPLC between *cis* and *trans* isomers of 4 resulted in values larger or close to the optimal value for 4a and for 4c. However, for the mixture B separation of *trans-4b* and *cis-4b* has R_s value high enough to recognize the components but very low to achieve an optimal resolution between the peaks. This behavior indicates that the polarity difference between *cis* and *trans* isomers of 4b is lower than the difference of polarity for isomers of 4a and 4c. For preparative LC separations, R_s between *cis* and *trans* isomers of 4 was not possible to measure because both isomers were overlapped. Different solvents and column lengths may be explored to achieve R_s values close to 1.5 between *trans-4*- and *cis-4* peaks.

4. CONCLUSION

Separation by LC was performed for a mixture of double-decker shaped silsesquioxanes functionalized with zero, one, and two hydroxyl groups. The presence of the polar group allowed different retention times for the mixtures evaluated including the *trans* and the *cis* isomers for the nanostructure functionalized with two hydroxyl groups. It was determined that adsorption of the nonpolar compound was neglectable because it migrates through the column without being retained.

Linear adsorption isotherms were identified for the structures dissolved in DCM. Highly concentrated solutions were not studied due to problems with the pump pistons and proximity to the detector limit. However, evaluation of larger concentrations may allow visualization of Langmuir type of isotherms. Nevertheless, linearity is an advantage for scale up of the separation process into a preparative column working in batch operations. HPLC was used to predict linear adsorption isotherm parameters that were further extrapolated to find adsorption isotherm parameters for commercially available silicas. These parameters allowed the prediction of collection intervals in large-scale columns.

Separations performed experimentally with the simulated parameters are accurate in the baseline of the chromatogram. But the peak shapes may require another type of isotherms predictive of tailing or perhaps competition. Other types of separation using this commercial stationary phase can be simulated with the adsorption parameters found in this work. In summary, this work proposes a simple predictive methodology for scale-up HPLC separations of side-capped octaphenyl double-decker shaped silsesquioxanes by the use of commercially available silica.

■ ASSOCIATED CONTENT

■ Supporting Information

The Supporting Information is available free of charge on the ACS Publications website at DOI: 10.1021/acs.iecr.8b05490.

Fraction analysis for separation of mixture B by HPLC; HPLC flow rate profile for preparatory column separating mixture C; fraction analysis for separation of mixture C by HPLC; and ^1H , ^{13}C and ^{29}Si NMR spectra for **2** [DDSQ-2((CH₃)₂)], **4a** [DDSQ-2((CH₃)-(OH))], **3a** [DDSQ-(CH₃)₂(CH₃)(OH)], **3b** [DDSQ-(CH₃)₂(CH₂CH₂)(OH)], and **3c** [DDSQ-(CH₃)₂(CH₂CH(CH₃)₂)(OH)] (PDF)

■ AUTHOR INFORMATION

Corresponding Authors

*REM: maleczka@chemistry.msu.edu, (517) 353-083.

*AL: leea@egr.msu.edu, (517) 355-5112.

ORCID

Robert E. Maleczka, Jr.: 0000-0002-1119-5160

Andre Lee: 0000-0001-6921-7214

Notes

The authors declare no competing financial interest.

■ ACKNOWLEDGMENTS

This work is support by the Office of Naval Research grant N00014-16-2109. We thank program manager Mr. William Nickerson for his support.

■ REFERENCES

(1) Ootake, N.; Yoshida, K. Organic Silicon Compound and Method for Producing Same, and Polysiloxane and Method for Producing Same. 20060155091:A1, July 13, 2006.

(2) Morimoto, Y.; Watanabe, K.; Ootake, N.; Inagaki, J.-I.; Yoshida, K.; Ohguma, K. Silsesquioxane Derivatives and Process for Production Thereof. 20040249103A1, December 9, 2004.

(3) Lee, D. W.; Kawakami, Y. Incompletely Condensed Silsesquioxanes: Formation and Reactivity. *Polym. J.* **2007**, *39*, 230–238.

(4) Mitula, K.; Duszczyk, J.; Brzakałski, D.; Dudzic, B.; Kubicki, M.; Marciniak, B. Tetra-Functional Double-Decker Silsesquioxanes as Anchors for Reactive Functional Groups and Potential Synthesis for Hybrid Materials. *Chem. Commun.* **2017**, *53*, 10370–10373.

(5) Schoen, B. W. *Aminophenyl Double Decker Silsesquioxanes: Spectroscopic Elucidation, Physical and Thermal Characterization, and Their Applications*; 2013.

(6) Schoen, B. W.; Holmes, D.; Lee, A. Identification and Quantification of Cis and Trans Isomers in Aminophenyl Double-Decker Silsesquioxanes Using ^1H – ^{29}Si gHMBC NMR. *Magn. Reson. Chem.* **2013**, *51*, 490–496.

(7) Schoen, B. W.; Lira, C. T.; Lee, A. Separation and Solubility of Cis and Trans Isomers in Nanostructured Double-Decker Silsesquioxanes. *J. Chem. Eng. Data* **2014**, *59*, 1483–1493.

(8) Seurer, B.; Vij, V.; Haddad, T.; Mabry, J. M.; Lee, A. Thermal Transitions and Reaction Kinetics of Polyhedral Silsesquioxane Containing Phenylethynylphthalimides. *Macromolecules* **2010**, *43*, 9337–9347.

(9) Kohri, M.; Matsui, J.; Watanabe, A.; Miyashita, T. Synthesis and Optoelectronic Properties of Completely Carbazole-Substituted Double-Decker-Shaped Silsesquioxane. *Chem. Lett.* **2010**, *39*, 1162–1163.

(10) Xu, S.; Zhao, B.; Wei, K.; Zheng, S. Organic-Inorganic Polyurethanes with Double Decker Silsesquioxanes in the Main Chains: Morphologies, Surface Hydrophobicity, and Shape Memory Properties. *J. Polym. Sci., Part B: Polym. Phys.* **2018**, *56*, 893–906.

(11) Wang, Z.; Yonggang, L.; Huijuan, M.; Wenpeng, S.; Tao, L.; Cuifen, L.; Junqi, N.; Guichun, Y.; Zuxing, C. Novel Phosphorus-Nitrogen-Silicon Copolymers with Double-Decker Silsesquioxane in the Main Chain and Their Flame Retardancy Application in PC/ABS. *Fire Mater.* **2018**, *2*, 16230.

(12) Liu, N.; Wei, K.; Wang, L.; Zheng, S. Organic-inorganic Polyimides with Double Decker Silsesquioxane in the Main Chains. *Polym. Chem.* **2016**, *7*, 1158–1167.

(13) Wei, K.; Wang, L.; Zheng, S. Organic-inorganic Polyurethanes with 3,13-Dihydroxypropyloctaphenyl Double-Decker Silsesquioxane Chain Extender. *Polym. Chem.* **2013**, *4*, 1491–1501.

(14) Hoque, M. A.; Kakihana, Y.; Shinke, S.; Kawakami, Y. Polysiloxanes with Periodically Distributed Isomeric Double-Decker Silsesquioxane in the Main Chain. *Macromolecules* **2009**, *42*, 3309–3315.

(15) Ervithayasuporn, V.; Sodkhomkhum, R.; Teerawatananond, T.; Phurat, C.; Phinyocheep, P.; Somsook, E.; Osotchan, T. Unprecedented Formation of Cis-and Trans-Di [(3-Chloropropyl) Isopropoxysilyl]-Bridged Double-Decker Octaphenylsilsesquioxanes. *Eur. J. Inorg. Chem.* **2013**, *2013*, 3292–3296.

(16) Walczak, M.; Januszewski, R.; Majchrzak, M.; Kubicki, M.; Dudzic, B.; Marciniak, B. Unusual Cis and Trans Architecture of Dihydrofunctional Double-Decker Shaped Silsesquioxane and Synthesis of Its Ethyl Bridged π -Conjugated Arene Derivatives. *New J. Chem.* **2017**, *41*, 3290–3296.

(17) Kucuk, A. C.; Matsui, J.; Miyashita, T. Langmuir-Blodgett Films Composed of Amphiphilic Double-Decker Shaped Polyhedral Oligomeric Silsesquioxanes. *J. Colloid Interface Sci.* **2011**, *355*, 106–114.

(18) Kucuk, A. C.; Matsui, J.; Miyashita, T. Synthesis and Photochemical Response of Ru(II)-Coordinated Double-Decker Silsesquioxane. *RSC Adv.* **2018**, *8*, 2148–2156.

(19) Espinas, J.; Pelletier, J. D. A.; Abou-Hamad, E.; Emsley, L.; Basset, J.-M. A Silica-Supported Double-Decker Silsesquioxane Provides a Second Skin for the Selective Generation of Bipodal Surface Organometallic Complexes. *Organometallics* **2012**, *31*, 7610–7617.

(20) Žak, P.; Dudzic, B.; Dutkiewicz, M.; Ludwiczak, M.; Marciniak, B.; Nowicki, M. A New Class of Stereoregular Vinylene-Arylene Copolymers with Double-Decker Silsesquioxane in the Main Chain. *J. Polym. Sci., Part A: Polym. Chem.* **2016**, *54*, 1044–1055.

(21) Liu, N.; Li, L.; Wang, L.; Zheng, S. Organic-Inorganic Polybenzoxazine Copolymers with Double Decker Silsesquioxanes in the Main Chains: Synthesis and Thermally Activated Ring-Opening Polymerization Behavior. *Polymer* **2017**, *109*, 254–265.

(22) Wu, S.; Hayakawa, T.; Kikuchi, R.; Grunzinger, S. J.; Kakimoto, M.-A.; Oikawa, H. Synthesis and Characterization of Semiaromatic Polyimides Containing POSS in Main Chain Derived from Double-Decker-Shaped Silsesquioxane. *Macromolecules* **2007**, *40*, 5698–5705.

(23) Hoque, M. A.; Kawakami, Y. Synthesis of Polysilsesquioxanes with Double-Decker Silsesquioxane Repeating Units. *J. Sci. Res.* **2016**, *8*, 217–227.

(24) Wu, S.; Hayakawa, T.; Kakimoto, M.-A.; Oikawa, H. Synthesis and Characterization of Organosoluble Aromatic Polyimides Containing POSS in Main Chain Derived from Double-Decker-Shaped Silsesquioxane. *Macromolecules* **2008**, *41*, 3481–3487.

(25) Vogelsang, D. F.; Dannatt, J. E.; Maleczka, R. E.; Lee, A. Separation of Asymmetrically Capped Double-Decker Silsesquioxanes Mixtures. *Polyhedron* **2018**, *155*, 189–193.

(26) Fornstedt, T.; Forssén, P.; Samuelsson, J. Chapter 18 - Modeling of Preparative Liquid Chromatography. In *Liquid Chromatography*; Fanali, S., Haddad, P. R., Poole, C. F., Schoenmakers, P., Lloyd, D., Eds.; Elsevier: Amsterdam, 2013; pp 407–425.

(27) Snyder, L. R.; Kirkland, J. J.; Dolan, J. W. *Introduction to Modern Liquid Chromatography*, 3rd ed.; Wiley: Hoboken, NJ, 2010.

(28) Gritti, F.; Guiochon, G. Systematic Errors in the Measurement of Adsorption Isotherms by Frontal Analysis Impact of the Choice of

Column Hold-up Volume, Range and Density of the Data Points. *J. Chromatogr. A* **2005**, *1097*, 98–115.

(29) Manual, I. *Agilent ChemStation for LC and CE Systems*.

(30) ASPEN. *Help File in ASPEN Chromatography V 10*; 2017.

(31) Vogelsang, D. F.; Maleczka, R. E.; Lee, A. HPLC Characterization of *cis* and *trans* mixtures of Double-Decker Shaped Silsesquioxanes. *Silicon* **2018** (online). DOI: [10.1007/s12633-018-0045-4](https://doi.org/10.1007/s12633-018-0045-4)